Arsenic trioxide inhibits the functions of lung fibroblasts derived from patients with idiopathic pulmonary fibrosis

Audrey Joannes, Claudie Morzadec, Maëla Duclos, Francisco Llamas Gutierrez, Dan Cristian Chiforeanu, Cécile Le Naoures, Bertrand de Latour, Simon Rouzé, Lutz Wollin, Stéphane Jouneau, et al.

▶ **To cite this version:**

Audrey Joannes, Claudie Morzadec, Maëla Duclos, Francisco Llamas Gutierrez, Dan Cristian Chiforeanu, et al.. Arsenic trioxide inhibits the functions of lung fibroblasts derived from patients with idiopathic pulmonary fibrosis. Toxicology and Applied Pharmacology, 2022, 441, pp.115972. 10.1016/j.taap.2022.115972 . hal-03629873

HAL Id: hal-03629873
https://hal.science/hal-03629873

Submitted on 12 Apr 2022

HAL is a multi-disciplinary open access archive for the deposit and dissemination of scientific research documents, whether they are published or not. The documents may come from teaching and research institutions in France or abroad, or from public or private research centers.

L'archive ouverte pluridisciplinaire **HAL**, est destinée au dépôt et à la diffusion de documents scientifiques de niveau recherche, publiés ou non, émanant des établissements d'enseignement et de recherche français ou étrangers, des laboratoires publics ou privés.

Distributed under a Creative Commons Attribution - NonCommercial 4.0 International License

Arsenic trioxide inhibits the functions of lung fibroblasts derived from patients with idiopathic pulmonary fibrosis.

Audrey Joannes[1,*], Claudie Morzadec[1], Maëla Duclos[1], Francisco Llamas Gutierrez[2], Dan Cristian Chiforeanu[2], Cécile Le Naoures[2], Bertrand De Latour[3], Simon Rouzé[3], Lutz Wollin[4], Stéphane Jouneau[1,5,$] and Laurent Vernhet[1,$]

[1]Univ Rennes, CHU Rennes, Inserm, EHESP, Irset (Institut de recherche en santé, environnement et travail) - UMR_S 1085, F-35000 Rennes, France.

[2]Department of pathology and cytology, Rennes University Hospital, 35033, Rennes, France;

[3]Department of Thoracic, cardiac and vascular surgery, Rennes University Hospital, 35033, Rennes, France;

[4]Boehringer Ingelheim Pharma GmbH & Co, KG, Biberach an der Riss, Germany;

[5]Department of Respiratory Diseases, Competence Center for Rare Pulmonary Disease, Rennes University Hospital, 35033, Rennes, France

[$] Equally contributed

* Corresponding author: Audrey Joannes: audrey.joannes@univ-rennes1.fr

ACCEPTED MANUSCRIPT - CLEAN COPY

Abstract

Idiopathic pulmonary fibrosis (IPF) is a chronic and fatal interstitial lung disease. Currently, no treatment can block or reverse the development of lung fibrosis in patients suffering from IPF. Recent studies indicate that arsenic trioxide (ATO), a safe, effective anti-cancer pro-oxidant drug, prevents the differentiation of normal human lung fibroblasts (NHLFs) *in vitro* and reduces experimental pulmonary fibrosis *in vivo*. In this context, we investigated the anti-fibrotic effects of ATO on the main fibrosis functions of human lung fibroblasts (HLFs) isolated from patients with IPF.

IPF and non-IPF (control) HLFs were incubated with 0.01-1 μM ATO and stimulated with pro-fibrotic factors (PDGF-BB or TGF-β1). We measured their rates of proliferation, migration and differentiation and the cell stress response triggered by ATO.

ATO did not affect cell viability but strongly inhibited the proliferation and migration of PDGF-BB-stimulated IPF and control HLFs. ATO also prevented myofibroblastic differentiation, as assessed by the expression of α-smooth muscle actin (α-SMA) and collagen-1, and the phosphorylation of SMAD2/3 in TGF-β1-stimulated HLFs. These antifibrotic effects were associated with increased expression of the transcription factor NRF2 and its target genes NQO1 and HMOX1. Genetic silencing of NRF2 inhibited the ATO-induced cell stress response but did not prevent the ATO-dependent inhibition of α-SMA expression in TGF-β1-stimulated HLFs.

The results demonstrate that ATO, at concentrations similar to exposure in blood plasma of ATO-treated cancer patients, counteracted pro-fibrotic activities of HLFs from IPF patients. We propose to consider ATO for clinical exploration to define the therapeutic potential in patients with IPF.

ACCEPTED MANUSCRIPT - CLEAN COPY

Keywords (6): Interstitial lung diseases, primary human lung fibroblasts, metalloid, proliferation, migration, differentiation.

Abbreviations: IPF: idiopathic pulmonary fibrosis, ILD: interstitial lung disease, PDGF-BB: platelet-derived growth factor BB, TGF-β1: transforming growth factor-β1, ATO: arsenic trioxide, HLFs: human lung fibroblasts, α-SMA: α-smooth muscle actin, APL: acute promyelocytic leukemia, COL1: collagen-1, NRF2: nuclear factor erythroid-2-related factor 2, NQO1: NADPH dehydrogenase quinone 1, HO-1: heme-oxygenase-1, MiRNA: microRNA, CDK: cyclin-dependent kinase, PBS: phosphate-buffered saline, ANOVA: one-way analysis of variance, SEM: standard error of the mean.

Journal Pre-proof

ACCEPTED MANUSCRIPT - CLEAN COPY

1. Background

Patients diagnosed with idiopathic pulmonary fibrosis (IPF), the most frequent idiopathic fibrosing interstitial lung disease (ILD), have an average life expectancy of 3-5 years (Lederer and Martinez, 2018; Raghu et al., 2018). Despite intensive research, the cellular and molecular mechanisms underlying the development of lung fibrosis remain unclear. The disease is probably triggered by repeated injuries to the alveolar epithelium, due to agents such as chronic cigarette smoking, viruses, or air pollutants. The resulting damage disturbes tissue repair and promotes abnormal fibroproliferation, myofibroblast differentiation and excessive collagen deposition eventually leading to chronic respiratory failure and death (Lederer and Martinez, 2018). Profibrotic mediators like transforming growth factor (TGF)-β and platelet-derived growth factor (PDGF), produced by epithelial, endothelial or infiltrating immune cells, play crucial roles in IPF pathogenesis by inducing the formation of fibroblastic foci (Budi et al., 2021; Grimminger et al., 2015). PDGF triggers the migration and proliferation of fibroblasts while TGF-β induces the differentiation of lung fibroblasts into myofibroblasts. These activated fibroblasts markedly express the α-smooth muscle actin (α-SMA) and produce abnormal amounts of collagen (Grimminger et al., 2015; Upagupta et al., 2018).

Nintedanib and pirfenidone are the only drugs that have been approved worldwide for treating IPF (Raghu et al., 2018). Low concentrations of these drugs decrease the proliferation and migration of human lung fibroblasts (HLFs) from IPF patients *in vitro.* Although high concentrations of them also prevent the differentiation of HLF into activated myofibroblasts, such concentrations are seldom reached in the plasma of treated patients (Conte et al., 2014; Hostettler et al., 2014; Rangarajan et al., 2016). The drugs reduce the progression of IPF by slowing the rate of lung function decline but they do not reverse lung fibrosis (King et al., 2014; Richeldi et al., 2020, 2014). Hence, new antifibrotic drugs are urgently required. Arsenic trioxide (ATO) has been approved for the treatment of acute promyelocytic leukemia

ACCEPTED MANUSCRIPT - CLEAN COPY

Journal Pre-proof

(APL) that is driven by the t(15:17) translocation (Kumana et al., 2002; Soignet et al., 2001). It is also being assessed for the management of solid tumors (Kim et al., 2020) and immunological disorders such as systemic lupus erythematosus (Hamidou et al., 2021). The concentrations of total arsenic measured in the plasma of patients treated with standard dosing (0.15 mg/kg/d, intravenous), immediately after the completion of administration and during the following hours, were in a range from 5-7 µM and 0.1-0.5 µM, respectively (Kumana et al., 2002; Shen et al., 2001, 1997). ATO administration is generally well tolerated but in few cases the treatment must be temporarily interrupted when adverse effects are observed and judged to be possibly related to ATO. Interestingly, experimental studies have demonstrated that these concentrations of ATO measured in the plasma of patients suffering from APL exhibit, *in vitro*, strong antifibrotic actions. ATO decreases the myofibroblast differentiation induced by TGF-β1 in both dermal and non-IPF HLFs *in vitro* (Luo et al., 2014; Zhong et al., 2019) and decreased the proliferation of ocular fibroblasts *in vitro* (Su et al., 2015). It attenuates both cisplatin-induced renal fibrosis in rats (Maghmomeh et al., 2020) and lung fibrosis in a murine model of systemic sclerosis *in vivo* (Kavian et al., 2012). Finally, ATO inhibits bleomycin-induced lung fibrosis in mice and rats by decreasing collagen deposition and inhibiting α-SMA expression (Gao et al., 2014; Luo et al., 2014).

ATO is a pro-oxidant metalloid that up-regulates the redox-sensitive expression of the transcription factor, NF-E2-related factor 2 (NRF2), in several cell types. NRF2 mediates the ATO-dependent stress response by stimulating the expression of several antioxidant genes. It also contributes to the arsenic effects on various major cell functions (Bourdonnay et al., 2009; Morales et al., 2009; Wang et al., 2012). In addition, increased NRF2 expression reduces the development of experimental lung fibrosis (Cho et al., 2004) and modulated the differentiation of HLF *in vitro* (Artaud-Macari et al., 2013).

ACCEPTED MANUSCRIPT - CLEAN COPY

This study was designed to determine whether ATO could inhibit the pro-fibrotic functions of HLFs from patients with IPF. We found that nanomolar concentrations of ATO, in the range of plasmatic concentrations achieved in APL patients treated with conventional ATO dosing, inhibited the proliferation and migration of HLFs from patients with IPF. In addition, independently of its ability to induce NRF2 expression ATO reduced the differentiation of fibroblasts to pro-fibrotic myofibroblasts.

ACCEPTED MANUSCRIPT - CLEAN COPY

2. Materials and Methods

2.1. Primary cultures of HLFs

IPF and control HLFs were isolated from lung tissue samples (Marchand-Adam et al., 2003). The IPF samples were from patients undergoing open lung biopsy (median age 68 year; range 51-77 years). IPF was diagnosed according to the ATS/ERS/JRS/ALAT criteria, including histopathological features of usual interstitial pneumonia (Raghu et al., 2018). Control samples were from cancer patients undergoing lobectomy or pneumonectomy, away from the tumor (median age 64.5 year; range 59-74 year). The absence of tumor tissue in control samples was verified histologically. This study was approved by the local ethics committee (Ethics Committee CHU Rennes, no 16123). Written informed consent was obtained from all subjects. All experiments were performed in accordance with relevant guidelines and regulations. Cell morphology was checked by phase contrast microscopy.

2.2. Cell culture and treatments

IPF (n=10) and control (n=6) HLFs were cultured in Dulbecco's Modified Eagle Medium (DMEM) (Gibco™, Life Technologies, Courtaboeuf, France) supplemented with 10% fetal calf serum (FCS) (Eurobio scientific, Evry, France), L-glutamine, antibiotic-antimycotic solution (Gibco™, Life Technologies) and used at passages 5 and 6. The HLFs used to analyze mRNA and protein expressions were seeded in 6-well plates for 24 h, and then starved in FCS-free DMEM for 16 h. TGF-β1-induced myofibroblast differentiation was measured by treating serum-starved HLFs with ATO (0.01-1 µM) (Formula: AS_2O_3, CAS number: 1327-53-3, molecular weight 197,84 g/mol; Sigma-Aldrich, St. Quentin Fallavier, France) for 24 h and then with TGF-β1 (1 ng/ml; Preprotech, Neuilly-sur-Seine, France) for 24 h. The HLFs used for cell growth and cell cycle analysis were serum-starved for 16 h, cultured in DMEM containing 1 % FCS and 0.01-1 µM ATO for 24 h, and finally stimulated with PDGF-BB (50 ng/ml) (R&D Systems, Bio-Techne, Lille, France) for a further 72 h. The

ACCEPTED MANUSCRIPT - CLEAN COPY

HLFs were treated with ATO for 24 h as this incubation time is enough to significantly modulate the phenotype of normal HLFs (Luo et al., 2014). The concentrations of ATO (0.01-1µM) were in a comparable range to the plasma concentrations that can be reached in APL patients treated with standard doses of ATO (Kumana et al., 2002; Shen et al., 2001, 1997).

2.3. Proliferation and viability

After ATO and PDGF-BB treatments, cells were dissociated with trysin, centrifugated (1500g, 5 min) and resuspended in DMEM containing 10 % FCS. Proliferation and viability were assessed with the acridine orange/propidium iodide staining (Logos Biosystems, Villeneuve d'Ascq, France) and an automated fluorescence cell counter (Luna™, Logos Biosystems). The cell viability dye causes viable nucleated cells to fluoresce green and nonviable nucleated cells to fluoresce red. After cell counting, the relative cell proliferation was calculated by dividing the number of viable cells exposed to ATO +/- PDGF-BB by the number of viable untreated cells arbitrarily set at 1. The cell viability was defined by dividing the number of viable cells by the number of viable and dead cells. It was expressed in percentages (%).

2.4. Cell cycle analysis

The HLFs used to analyse the cell cycle distribution were fixed in ice-cold 70 % (v/v) ethanol for 30 min at 4°C, and collected by centrifugation (900g/5 min). The cell pellets were washed, suspended in PBS (pH 7.4) containing propidium iodide (50 µg/mL) and DNase-free RNase A (100 µg/mL) (Sigma-Aldrich, St. Quentin Fallavier, France) and incubated at 4°C for 1 h. DNA was quantified by flow cytometry using an LRSFortessa™X20 flow cytometer (BD Biosciences, Paris, France). Data were analysed with flow cytometry data analysis software FlowLogic (Miltenyi Biotech, Paris, France) using the Watson improved method.

ACCEPTED MANUSCRIPT - CLEAN COPY

2.5. Migration assay

HLF migration was assessed in a modified Boyden chamber assay, using a Transwell permeable support (6.5 mm, 8 μm) (Corning, Tewksbury, MA, USA) coated with fibronectin (0.1 μg/ml) (Sigma-Aldrich, St. Quentin Fallavier, France). The medium in the upper compartment (DMEM-0%FCS) contained 0.01-1μM ATO and that in the lower compartment contained (DMEM-1%FCS) 25 ng/ml PDGF-BB. Cells were incubated for 24 h at 37°C, fixed in 70 % ethanol, and labelled with DAPI. Migration was assessed by counting the number of cells on the lower surface of the filters. The relative cell migration was defined by dividing the number of migrating cells stimulated with PDGF-BB by the number of migrating cells left untreated and arbitrarily set at 1.

2.6. siRNA transfection

HLFs were transfected for 8 h with 25 nM Nrf2 siRNA (NM_006164) (Dharmacon SMARTpool siRNA reagents, Fisher Scientific, Illkirch, France), or negative control (scramble) siRNA (D-001810-10-20, Dharmacon, plus non-targeting pool) using Lipofectamine RNAiMAX Reagent (Invitrogen, Thermo Fisher scientific) according to the manufacturer's instructions. Treated cells were starved, incubated with 1 μM ATO for 24 h and stimulated with 1 ng/ml TGF-β1 for a further 24 h.

2.7. Protein analysis

HLFs were lysed in ice-cold RIPA buffer containing cOmplete™ Protease Inhibitor Cocktail (Roche, Sigma-Aldrich) and phosphatase inhibitor cocktail (Sigma-Aldrich). Proteins were separated by electrophoresis on 10 % Tris-glycine SDS polyacrylamide gels and transferred to nitrocellulose membranes (pore size: 0.2 μm, Invitrogen). Free binding sites were blocked by incubation in 5 % milk or bovine serum albumin (BSA) (Sigma-Aldrich, St. Quentin

ACCEPTED MANUSCRIPT - CLEAN COPY

Fallavier, France) for 2 h at room temperature. Membranes were then incubated with the appropriate primary human antibody (Ab) overnight at 4°C. The primary Abs were anti-α-SMA (clone 1A4, Sigma-Aldrich), anti-collagen I (Southern Biotechnology Associates, Birmingham, AL), anti-NRF2 (ab62352, abcam, Amsterdam, Netherlands), anti-NADPH-quinone-oxydoreductase-1 (NQO1) (sc-271116, Santa Cruz, Santa Cruz, USA), anti-heme oxygenase-1 (HO-1) (ADI-SPA-895, Enzo Life Science, NY, USA), and anti-GAPDH (mab90009-P, Covalab, Bron, France) Abs. Anti-phospho p44/42 MAPK (197G2), anti-p44/42 MAPK (9101), anti-phospho SMAD2 (3104), anti-SMAD2 (D43B4), anti-phospho SMAD3 (C25A9), anti-SMAD3 (C67H9), anti-phospho PDGF receptor (PDGFR) β (3161) and anti-PDGFR (28E1) Abs were from Cell Signaling Technology (Massachusetts, USA). Digital images were acquired on a gel imaging system (Chemi doc, BIO-RAD Laboratories, Marnes-La-Coquette, France) equipped with a CCD camera. Western blots were quantified by densitometry using Image Lab™ software (BIO-RAD) and normalized to GAPDH. The relative protein expression in stimulated cells was determined by arbitrarily setting at 1 the protein expression measured in untreated cells.

2.8. RNA isolation and RT-PCR assays

Total RNAs were extracted using the mRNA extraction kit from Macherey Nagel (Hoerdt, France) according to the manufacturer's instructions. RNA concentrations were measured by spectrofluorimetry using a NanoDrop 1000 (Thermo Fisher scientific, Saint-Herblain, France) and were in a range of 23.6 to 183.2 ng/ml. The purity (260/280 ratio) of each RNA sample was between 2 and 2.2. mRNAs were reverse transcribed using the High-Capacity cDNA Reverse Transcription kit (Applied Biosystems, Thermo Fisher Scientific). Quantitative PCR (polymerase chain reaction) was performed using the SYBR Green methodology on a CFX384 Real-Time PCR System (Bio-Rad Laboratories) in duplicates. All the primers were provided by Sigma-Aldrich (KiCqStart™ SYBR® Green Primers, St. Quentin Fallavier,

ACCEPTED MANUSCRIPT - CLEAN COPY

France). The specificity of gene amplification was checked at the end of PCR using the comparative cycle threshold method (CFX Manager Software). The mean Cq values were used to normalize the target mRNA concentrations to those of the 18S ribosomal protein by the $2^{(-\Delta\Delta Cq)}$ method. The relative mRNA expression was defined by the ratio between the treated conditions compared to the untreated condition which was arbitrarily set at 1.

2.9. Statistical analysis

All results are presented as means ± standard errors of mean (SEM) of the indicated numbers of independent biological experiments. All biological experiments were performed with different primary cell cultures. Statistical analyses were performed with Prism 5 (GraphPad Software, La Jolla, CA). Significant differences were determined by Student's *t*-test ($ $p<0.05$; $$ $p<0.01$; $$$ $p<0.001$) when two groups were compared, or by ANOVA followed by the Dunnett's Multiple comparison *t*-test (* $p<0.05$; ** $p<0.01$; *** $p<0.001$) for more than 2 groups.

ACCEPTED MANUSCRIPT - CLEAN COPY

3. Results

3.1. ATO inhibited PDGF-BB-induced proliferation of IPF and control HLFs

Fibroblast proliferation is a major contributor to the formation of fibroblastic foci in the lungs of IPF patients (King et al., 2011). IPF and control cells were cultured with ATO for 72 h to determine the effects of ATO on basal HLF growth. ATO did not alter the viability of HLF under these conditions (supplemental Fig. 1A and 1B) or reduce the proliferation of IPF HLFs (Fig. 1A) although 1 μM ATO significantly decreased the basal growth of control cells (Fig. 1B). Cell proliferation in lung fibrosis is stimulated by several pro-fibrotic cytokines, particularly by PDGF-BB. We therefore investigated the capacity of ATO to prevent the proliferative effects of PDGF-BB. ATO-treated IPF and control HLFs were incubated with PDGF-BB for 72 h. As expected, PDGF-BB significantly increased the proliferation of both IPF and control HLFs (Fig. 1C-1D). ATO did not reduce the viability of these activated HLFs (supplemental Fig. 1C and 1D) but attenuated the PDGF-BB-induced proliferation in a concentration-dependent manner (Fig. 1C-1D); the effect was numerically detectable at 0.01 μM and it was maximal at 0.3 μM in IPF HLF and at 1 μM in control HLF.

3.2. ATO modified the cell cycle of IPF and control HLFs.

We next determined the influence of ATO on the cell cycle of PDGF-BB-stimulated HLFs. As shown in the representative pictures displayed in Figure 2A, after 72 h, most IPF HLFs were in the G0/G1 phase whatever their treatment. ATO significantly decreased the percentage of IPF HLFs arrested in G0/G1 while it markedly increased the percentage of cells in G2/M phase after a 72 h-incubation with PDGF-BB (Fig. 2B). It had a similar effect on the cell cycle distribution of activated control HLFs (supplemental Fig. 2A and 2B). The third set of experiments examined the capacity of ATO to modulate cell cycle progression by altering the expression of cell cycle regulatory proteins. PDGF-BB increased the expressions of the cyclin D1/CDK4, cyclin A/CDK2 and cyclin B/CDK1 that control progression in the G1, S

ACCEPTED MANUSCRIPT - CLEAN COPY

and G2 phases, respectively (Figure 2C-2D). At 1 μM, ATO had no effect on cyclin D1 concentration while it slightly decreased the expressions of its CDK4 partner. It also significantly reduced the expression of cyclin A/CDK2 and cyclin B (Figure 2C-2D).

3.3. ATO prevented the PDGF-BB-induced migration of IPF and control HLFs.

Fibroblast migration is another important step in the formation of fibroblastic foci (Chilosi et al., 2006; King et al., 2011). PDGF-BB not only stimulates cell proliferation, its potent chemoattractant properties also promote fibrogenesis in pulmonary tissues. We found that it significantly increased the migration of IPF and control HLFs and that ATO reduced in a concentration-dependent manner, the response of both IPF and control HLFs to PDGF-BB stimulation (Figure 3). Its effect reached significance at 0.1 μM and maximum at 1 μM; 1 μM ATO almost totally blocked the PDGF-BB-induced migration of IPF HLFs.

3.4. ATO reduced PDGF-BB-induced phosphorylation of p38-kinase.

We next determined if ATO could prevent the growth and migration of IPF HLFs through inhibition of the PDGF-BB signaling by determining its effects on the phosphorylation of the kinases induced by PDGF receptor (PDGFR) activation. As shown in Figures 4A and 4B, PDGF-BB increased the levels of phosphorylated PDGFR, ERK, AKT and p38-kinase. ATO had no effect on the phosphorylation of PDGFR, ERK and AKT but it significantly decreased the phosphorylation of p38-kinase at 1μM.

3.5. ATO modulated the TGFβ-1-induced differentiation of HLFs.

Activation of the TGF-β pathway drives the differentiation of fibroblasts to myofibroblasts and is therefore an essential feature of fibrosis (Budi et al., 2021). We examined the capacity of ATO to prevent the TGF-β1-dependent differentiation of IPF and control HLFs by first determining the effects of ATO on the mRNA levels of two major pro-fibrosis genes, COL1A1 and ACTA2. IPF and control HLFs were incubated with 1 ng/ml TGF-β1 for 24 h, which increased the concentrations of *COL1A1* and *ACTA2* mRNA levels (Supplemental

ACCEPTED MANUSCRIPT - CLEAN COPY

Figure 3). ATO did not prevent the increase in *COL1A1* mRNA in IPF HLFs but it significantly reduced the increase in *ACTA2* mRNA in these cells (Supplemental Figure 3A-3B). In contrast, it did not prevent the increase in this profibrotic gene expression in control HLFs (Supplemental Figure 3D). ATO had no effect on the basal expression of COL-1 and α-SMA proteins in HLFs (Supplemental Figure 4). However, as shown in the Figures 5A-5D, ATO reduced, in a concentration dependent manner, the expression of COL-1 and α-SMA protein levels in both IPF and control HLFs stimulated with TGF-β1.

Because activation of the SMAD2 and SMAD3 pathways plays a key role in the action of TGF-β1, we next examined the capacity of ATO to prevent fibroblast differentiation by inhibiting the phosphorylation of SMAD proteins. TGF-β1 stimulated the phosphorylation of phospho-SMAD2 and phospho-SMAD3 proteins in IPF and control HLFs (Figures 6). ATO significantly reduced the levels of these phosphorylated proteins at its highest concentration (1 μM) in IPF HLFs (Figures 6A-6B) but it decreased only the level of phosphorylated SMAD3 in control cells (Figures 6C-6D).

3.6. ATO induced NRF2 and antioxidant protein expression in IPF and control HLFs.

ATO can modulate cell functions by increasing the expression of the redox-sensitive transcription factor NRF2 (Bourdonnay et al., 2009; Wang et al., 2012). NRF2 not only controls the cell stress responses but it also limits the development of lung fibrosis by interfering with the TGF-β1 signaling (Artaud-Macari et al., 2013; Gong and Yang, 2020). Thus, we next determined if NRF2 could mediate, at least in part, the antifibrotic effects of ATO on IPF and control HLFs. To this goal, we first studied the impact of ATO on NRF2 expression. Most cell types contain low concentrations of NRF2 because it is bound to Keap1 that promotes its ubiquitination by Cul3 ubiquitin ligase and its rapid degradation by the proteasome. The oxidation of cysteine residues in Keap1 that occurs in cell stress reduces the

ACCEPTED MANUSCRIPT - CLEAN COPY

interaction of NRF2 with Cul3, so preventing its ubiquitination and subsequent degradation (He and Ma, 2009). Stabilized NRF2 protein moves into the nuclei during cell stress, where it promotes the expression of several antioxidant genes. We measured the influence of ATO on NRF2 protein stabilization and the cell stress response in HLFs. As frequently observed in other cell types (Bourdonnay et al., 2009), ATO rapidly increased the concentration of NRF2 protein in IPF HLFs (Fig. 7A); the maximum response was obtained after incubation with 0.5 μM ATO for 1 h (Fig. 7B). We next measured the activities of the antioxidant genes NQO1 and HMOX1, which encode proteins NQO1 and HO-1, as they are induced by NRF2 in many cell types. ATO dose-dependently increased the concentrations of NQO1 and HO-1 in unstimulated and TGF-β1-stimulated IPF HLFs (Figures 7C-7F). Maximal effects were detected in cells treated with 1 μM ATO. TGF-β1 had no significant effect on the expression of these proteins. ATO similarly stabilized NRF2 and stimulated NQO1 and HO-1 synthesis in control HLFs (Supplemental Fig. 5).

3.7. NRF2 did not mediate the ATO-dependent inhibition of TGF-β1-induced myofibroblast differentiation in IPF HLF.

In a last of experiments, we examined the contribution of NRF2 to the inhibition of the TGF-β-dependent differentiation of IPF HLFs induced by ATO. We inhibited NRF2 gene expression using SiRNA technology. Both unstimulated and TGF-β1-stimulated IPF cells transfected with NRF2 SiRNA had decreased *NRF2* mRNA levels whether or not they were cultured in the presence of ATO (Fig. 8A). NRF2 gene silencing also significantly decreased the concentration of basal *NQO1* mRNA in unstimulated cell and prevented any increase in stimulated cells that had been treated with ATO (Fig. 8B). However, this treatment neither reduced the induction of *ACTA2* mRNA by TGF-β1 nor blocked the inhibition of α-SMA protein expression by ATO in TGF-β1-stimulated IPF HLFs (Fig. 8C).

ACCEPTED MANUSCRIPT - CLEAN COPY

4. Discussion

Our results indicate that ATO inhibits major profibrotic processes in primary HLFs from both IPF and normal lung tissue. It inhibits the proliferation and migration of PDGF-BB-stimulated HLFs and reduces the myofibroblast differentiation induced by TGF-β1. ATO also triggers a stress response controlled by the NRF2 transcription factor in IPF HLF. However, inhibiting NRF2 synthesis did not block the antifibrotic effects of ATO on TGF-β1-stimulated HLFs.

We first showed that ATO had little or no effects on the proliferation of unstimulated IPF and control HLFs but that non-cytotoxic concentrations (0.1 - 1 µM) significantly inhibited the proliferation of both IPF and control HLFs stimulated with PDGF-BB. This growth factor plays a major role in lung fibrosis by promoting the formation of fibroblastic foci (Bonner, 2004). Its concentration is increased in murine models of lung fibrosis (Zhuo et al., 2004) and inhibiting PDGF signaling markedly reduces pulmonary fibrosis in mice treated with bleomycin (Aono et al., 2005). We have not identified the molecular mechanism by which ATO reduced HLF proliferation but we have shown that it modulates the cell cycle in PDGF-BB-stimulated HLFs. It significantly reduced the percentages of cells in the G0-G1 phase and greatly increased those arrested in G2/M. These findings suggest that ATO does not alter DNA synthesis but rather prevents the entry of HLFs into mitosis. ATO is known to disturb the cell cycle by modulating the expression of cyclin and CDK (Liu et al., 2015; Park et al., 2001; Su et al., 2015; Zhao et al., 2002). In HLF ATO did not alter the concentration of cyclin-D1, which controls the G0 to G1 progression, but it decreased the concentrations of cyclin-A, cyclin-B and CDK2, all key regulators of the G2/M phase transition, so retarding mitosis.

ACCEPTED MANUSCRIPT - CLEAN COPY

We also found that increasing concentrations of ATO greatly reduced the migration of PDGF-BB-stimulated IPF and control HLFs. This is relevant in the pathogenesis of the disease because IPF fibroblasts have increased capacity for migration and invasion, making them more destructive in lung tissue (Suganuma et al., 1995). ATO inhibits the migration of several cell types, including vascular endothelial (Yang et al., 2017) , glioblastoma (Ghaffari et al., 2016), hepatocellular carcinoma (Zhang et al., 2020), cervical (Wei et al., 2005), and breast cancer cells (Zhang et al., 2016). However, its effect on the migration of HLFs had never been reported. ATO seems to reduce cell migration by several molecular mechanisms. It impairs the polymerization of microtubules (Gao et al., 2020), decreases the concentrations of the matrix metalloproteinases MMP-2 and MMP-9 (Zhang et al., 2018), modulates the concentrations of certain mi-RNAs (Shi et al., 2017; Zhang et al., 2016), and interferes with key signalling pathways triggered by vascular endothelial growth factor, basic fibroblast growth factor receptor, and PDGF (Tingting et al., 2010; Yang et al., 2017). We found that ATO specifically reduced the phosphorylation of p38-kinase in PDGF-stimulated HLFs. This kinase promotes the cell proliferation and migration induced by PDGF (Tangkijvanich et al., 2002; Yamaguchi et al., 2001) and can contribute to lung fibrogenesis (Matsuoka et al., 2002). It will be interesting to determine whether inhibiting p38-kinase prevents the proliferation and/or migration of PDGF-stimulated IPF HLFs in order to further understand these antifibrotic effects of ATO.

The TGF-β-dependent differentiation of fibroblasts to myofibroblasts is an important pathogenic event in IPF fibrogenesis as myofibroblasts produce excess extracellular matrix leading to lung tissue stiffness (Budi et al., 2021). We found that ATO significantly decreased the TGF-β1-dependent synthesis of the myofibroblastic markers α-SMA and collagen-1 by HLFs, probably by blocking the activation of SMAD2/3. This agrees well with reports describing its impact on animal models of fibrosis. ATO was shown to decrease the

ACCEPTED MANUSCRIPT - CLEAN COPY

development of pulmonary fibrosis and myofibroblastic marker concentrations in mice and rats treated with bleomycin (Gao et al., 2014; Luo et al., 2014). It also limits dermal thickening and inhibits collagen deposition in a mouse model of systemic sclerosis (Kavian et al., 2012). However, ATO can promote fibrosis in organs such as heart and liver by increasing TGF-β1 synthesis or TGF-β1 signaling in chronically exposed animals (Chu et al., 2012; Dai et al., 2019).

In our latest experiments, we found an association between the antifibrotic effects of ATO with a stress response controlled by the transcription factor NRF2. NRF2-dependent expression of the HMOX1 and NQO1 genes was rapidly induced in ATO-treated HLF that had been stimulated with TGF-β1 or left unstimulated. We thus hypothesized that NRF2 activation could mediate, at least in part, the ATO-dependent inhibition of TGF-β1 effects in HLF. There is some support for this hypothesis. NRF2-deleted mice develop more severe pulmonary fibrosis in response to bleomycin (Cho et al., 2004), whereas NRF2 inducers, such as sulforaphane and esomeprazole, attenuate fibrotic responses in vitro and/or vivo by activating the NRF2 pathway (Artaud-Macari et al., 2013; Ebrahimpour et al., 2021). NRF2 notably reduces the TGF-β-dependent production of reactive oxygen species by controlling the synthesis of antioxidant proteins; the generation of reactive oxygen species reinforces the TGF-β signaling and its subsequent profibrotic effects in several models (Guan et al., 2018; Yang et al., 2013). Other studies indicate that NRF2 is a major molecular mediator of the antifibrotic response and that stimulating its synthesis could be a novel strategy for limiting fibrosis (Oh et al., 2012; Wei et al., 2017). Unfortunately, our results do not support this. Blocking NRF2 synthesis by genetic silencing clearly inhibited NQO1 expression but not that of α-SMA in TGF-β1-stimulated HLFs cultured with or without ATO. Other molecular mechanisms must therefore drive the ATO-dependent inhibition of TGF-β1 affects. For example, the reduction in phosphorylated SMAD3 concentrations in normal HLFs exposed to

ACCEPTED MANUSCRIPT - CLEAN COPY

elemental arsenic is correlated with a concomitant decrease in promyelocytic leukemia (PML) nuclear bodies and PML protein. PML knock-out mouse embryonic fibroblasts produce lower concentrations of fibrotic markers in response to TGF-β1 (Luo et al., 2014). Arsenic inhibits TGF-β1 signaling in human cancer cells by improving the expression of microRNA-155, which could contribute to experimental fibrosis and IPF (Ji et al., 2014; Kurowska-Stolarska et al., 2017). Additional experiments are required to determine whether such molecular mechanisms are involved in the antifibrosis effects of ATO on IPF HLFs.

Our results indicate that ATO reduces the proliferation, migration and differentiation of IPF HLF, as reported for nintedanib and pirfenidone, the two drugs approved for the treatment of IPF. At low nanomolar concentrations, nintedanib binds to the ATP binding pocket of various growth factor receptors, including the PDGF-BB receptor, resulting in the inhibition of the receptor autophosphophorylation and the downstream signaling cascades that control proliferation and migration (Hostettler et al., 2014; Wollin et al., 2015). At micromolar concentration, nintedanib can also prevent the differentiation of HLFs by inhibiting the activation of the TGF-β receptor (Rangarajan et al., 2016). However, such concentrations are rarely achieved in the plasma of IPF patients treated with standard dosing of nintedanib. Pirfenidone, a synthetic small-molecule deriving from pyridone, exerts antifibrotic effects by molecular mechanisms that remain still unclear. Although it can interfere with the TGF-β and PDGF-BB signaling, its molecular targets have not been identified yet (Conte et al., 2014; Ruwanpura et al., 2020). Pirfenidone can also reduce the production of oxygen activated species and limit inflammatory processes (Plataki et al., 2019). The antifibrotic effects of pirfenidone are induced *in vitro* at concentrations that are generally much higher than those measured in the plasma of IPF patient treated with standard drug dosing (Barranco-Garduño et al., 2020). The present study shows that ATO can block proliferation, migration and differentiation of HLFs at non-cytotoxic concentrations that can be reached in the plasma of

ACCEPTED MANUSCRIPT - CLEAN COPY

APL patients treated with ATO (0.15 mg/kg) (Kumana et al., 2002; Shen et al., 2001; Soignet et al., 2001). These antifibrotic effects of ATO might thus occur in patients with IPF treated with a similar dosing. Unexpectedly, the ATO concentrations used in our study were very different from those inhibiting the myofibroblastic differentiation of normal HLFs in a previous study (Luo et al., 2014). These authors showed that nanomolar concentrations (10-20 nM) of ATO inhibited TGF-β1-induced α-SMA and COL-1 synthesis while we found that these low concentrations have no effect on the phenotype of HLFs. The difference may arise from the commercial batches of normal HLFs used by Luo et al. The response of HLFs to ATO may therefore vary from one patient to another.

5. Conclusion

We demonstrate that non-cytotoxic concentrations of ATO have potent antifibrotic effects in IPF HLFs. This suggests that ATO should be considered for exploration of the therapeutic potential in patients with IPF.

6. Ethics approval and consent to participate

This study was approved by the Ethics Committee of CHU Rennes, no 16123. Written informed consent was obtained from all subjects.

7. Availability of data and materials

The datasets supporting the conclusions of this article are included in the article and its additional files.

8. Competing interests

SJ has received fees, funding or reimbursement for national and international conferences, boards, expert or opinion groups, research projects over the past 5 years from Actelion, AIRB, Astra Zeneca, Bellorophon Therapeutics, Biogen, BMS, Boehringer Ingelheim, Chiesi,

ACCEPTED MANUSCRIPT - CLEAN COPY

Fibrogen, Galecto Biotech, Genzyme, Gilead, GSK, LVL, Mundipharma, Novartis, Olam Pharm, Pfizer, Pliant Therapeutics, Roche, Sanofi, Savara-Serendex. AJ and LV report grants from Boehringer Ingelheim.

LW is an employee of Boehringer Ingelheim.

The other authors declare that they have no competing interests.

9. Funding

This work was supported by The Institut National de la Santé et de la Recherche Médicale (INSERM), the Université de Rennes (Univ Rennes) and Boehringer Ingelheim Pharma GmbH.

10. Authors' contributions

LV, SJ, AJ conceived and designed the study. AJ, CM, MD performed the experiments. AJ, LV, SJ analyzed and interpreted the data. FLG, DCC, CLN, BDLT, SR provided lung biopsy. AJ, LV, SJ, LW wrote the paper. All authors read and approved the final manuscript.

11. Acknowledgements

We thank Dr Owen Parkes for editing the English text.

Supplementary data

Supplementary material

12. References

Aono, Y., Nishioka, Y., Inayama, M., Ugai, M., Kishi, J., Uehara, H., Izumi, K., Sone, S., 2005. Imatinib as a novel antifibrotic agent in bleomycin-induced pulmonary fibrosis in mice. Am. J. Respir. Crit. Care Med. 171, 1279–1285. https://doi.org/10.1164/rccm.200404-531OC

ACCEPTED MANUSCRIPT - CLEAN COPY

Artaud-Macari, E., Goven, D., Brayer, S., Hamimi, A., Besnard, V., Marchal-Somme, J., Ali, Z.E., Crestani, B., Kerdine-Römer, S., Boutten, A., Bonay, M., 2013. Nuclear factor erythroid 2-related factor 2 nuclear translocation induces myofibroblastic dedifferentiation in idiopathic pulmonary fibrosis. Antioxid. Redox Signal. 18, 66–79. https://doi.org/10.1089/ars.2011.4240

Barranco-Garduño, L.M., Buendía-Roldan, I., Rodriguez, J.J., González-Ramírez, R., Cervantes-Nevárez, A.N., Neri-Salvador, J.C., Carrasco-Portugal, M.D.C., Castañeda-Hernández, G., Martinez-Espinosa, K., Selman, M., Flores-Murrieta, F.J., 2020. Pharmacokinetic evaluation of two pirfenidone formulations in patients with idiopathic pulmonary fibrosis and chronic hypersensitivity pneumonitis. Heliyon 6, e05279. https://doi.org/10.1016/j.heliyon.2020.e05279

Bonner, J.C., 2004. Regulation of PDGF and its receptors in fibrotic diseases. Cytokine Growth Factor Rev. 15, 255–273. https://doi.org/10.1016/j.cytogfr.2004.03.006

Bourdonnay, E., Morzadec, C., Fardel, O., Vernhet, L., 2009. Redox-sensitive regulation of gene expression in human primary macrophages exposed to inorganic arsenic. J. Cell. Biochem. 107, 537–547. https://doi.org/10.1002/jcb.22155

Budi, E.H., Schaub, J.R., Decaris, M., Turner, S., Derynck, R., 2021. TGF-β as a driver of fibrosis: physiological roles and therapeutic opportunities. J. Pathol. https://doi.org/10.1002/path.5680

Chilosi, M., Zamò, A., Doglioni, C., Reghellin, D., Lestani, M., Montagna, L., Pedron, S., Ennas, M.G., Cancellieri, A., Murer, B., Poletti, V., 2006. Migratory marker expression in fibroblast foci of idiopathic pulmonary fibrosis. Respir. Res. 7, 95. https://doi.org/10.1186/1465-9921-7-95

Cho, H.-Y., Reddy, S.P.M., Yamamoto, M., Kleeberger, S.R., 2004. The transcription factor NRF2 protects against pulmonary fibrosis. FASEB J. Off. Publ. Fed. Am. Soc. Exp. Biol. 18, 1258–1260. https://doi.org/10.1096/fj.03-1127fje

Chu, W., Li, C., Qu, X., Zhao, D., Wang, X., Yu, X., Cai, F., Liang, H., Zhang, Y., Zhao, X., Li, B., Qiao, G., Dong, D., Lu, Y., Du, Z., Yang, B., 2012. Arsenic-induced interstitial myocardial fibrosis reveals a new insight into drug-induced long QT syndrome. Cardiovasc. Res. 96, 90–98. https://doi.org/10.1093/cvr/cvs230

Conte, E., Gili, E., Fagone, E., Fruciano, M., Iemmolo, M., Vancheri, C., 2014. Effect of pirfenidone on proliferation, TGF-β-induced myofibroblast differentiation and fibrogenic activity of primary human lung fibroblasts. Eur. J. Pharm. Sci. Off. J. Eur. Fed. Pharm. Sci. 58, 13–19. https://doi.org/10.1016/j.ejps.2014.02.014

Dai, J., Xu, M., Zhang, X., Niu, Q., Hu, Y., Li, Y., Li, S., 2019. Bi-directional regulation of TGF-β/Smad pathway by arsenic: A systemic review and meta-analysis of in vivo and in vitro studies. Life Sci. 220, 92–105. https://doi.org/10.1016/j.lfs.2019.01.042

Ebrahimpour, A., Wang, M., Li, L., Jegga, A.G., Bonnen, M.D., Eissa, N.T., Raghu, G., Jyothula, S., Kheradmand, F., Hanania, N.A., Rosas, I.O., Ghebre, Y.T., 2021. Esomeprazole attenuates inflammatory and fibrotic response in lung cells through the MAPK/Nrf2/HO1 pathway. J. Inflamm. Lond. Engl. 18, 17. https://doi.org/10.1186/s12950-021-00284-6

Gao, L., Xue, B., Xiang, B., Liu, K.J., 2020. Arsenic trioxide disturbs the LIS1/NDEL1/dynein microtubule dynamic complex by disrupting the CLIP170 zinc finger in head and neck cancer. Toxicol. Appl. Pharmacol. 403, 115158. https://doi.org/10.1016/j.taap.2020.115158

ACCEPTED MANUSCRIPT - CLEAN COPY

Gao, S.-Y., Zhou, X., Li, Y.-J., Liu, W.-L., Wang, P.-Y., Pang, M., Xie, S.-Y., Lv, C.-J., 2014. Arsenic trioxide prevents rat pulmonary fibrosis via miR-98 overexpression. Life Sci. 114, 20–28. https://doi.org/10.1016/j.lfs.2014.07.037

Ghaffari, S.H., Yousefi, M., Dizaji, M.Z., Momeny, M., Bashash, D., Zekri, A., Alimoghaddam, K., Ghavamzadeh, A., 2016. Arsenic Trioxide Induces Apoptosis and Incapacitates Proliferation and Invasive Properties of U87MG Glioblastoma Cells through a Possible NF-κB-Mediated Mechanism. Asian Pac. J. Cancer Prev. APJCP 17, 1553–1564. https://doi.org/10.7314/apjcp.2016.17.3.1553

Gong, Y., Yang, Y., 2020. Activation of Nrf2/AREs-mediated antioxidant signalling, and suppression of profibrotic TGF-β1/Smad3 pathway: a promising therapeutic strategy for hepatic fibrosis - A review. Life Sci. 256, 117909. https://doi.org/10.1016/j.lfs.2020.117909

Grimminger, F., Günther, A., Vancheri, C., 2015. The role of tyrosine kinases in the pathogenesis of idiopathic pulmonary fibrosis. Eur. Respir. J. 45, 1426–1433. https://doi.org/10.1183/09031936.00149614

Guan, Y., Tan, Y., Liu, W., Yang, J., Wang, D., Pan, D., Sun, Y., Zheng, C., 2018. NF-E2-Related Factor 2 Suppresses Intestinal Fibrosis by Inhibiting Reactive Oxygen Species-Dependent TGF-β1/SMADs Pathway. Dig. Dis. Sci. 63, 366–380. https://doi.org/10.1007/s10620-017-4710-z

Hamidou, M., Néel, A., Poupon, J., Amoura, Z., Ebbo, M., Sibilia, J., Viallard, J.-F., Gaborit, B., Volteau, C., Hardouin, J.B., Hachulla, E., Rieger, F., 2021. Safety and efficacy of low-dose intravenous arsenic trioxide in systemic lupus erythematosus: an open-label phase IIa trial (Lupsenic). Arthritis Res. Ther. 23, 70. https://doi.org/10.1186/s13075-021-02454-6

He, X., Ma, Q., 2009. NRF2 Cysteine Residues Are Critical for Oxidant/Electrophile-Sensing, Kelch-Like ECH-Associated Protein-1-Dependent Ubiquitination-Proteasomal Degradation, and Transcription Activation. Mol. Pharmacol. 76, 1265–1278. https://doi.org/10.1124/mol.109.058453

Hostettler, K.E., Zhong, J., Papakonstantinou, E., Karakiulakis, G., Tamm, M., Seidel, P., Sun, Q., Mandal, J., Lardinois, D., Lambers, C., Roth, M., 2014. Anti-fibrotic effects of nintedanib in lung fibroblasts derived from patients with idiopathic pulmonary fibrosis. Respir. Res. 15, 157. https://doi.org/10.1186/s12931-014-0157-3

Ji, H., Li, Y., Jiang, F., Wang, X., Zhang, J., Shen, J., Yang, X., 2014. Inhibition of transforming growth factor beta/SMAD signal by MiR-155 is involved in arsenic trioxide-induced anti-angiogenesis in prostate cancer. Cancer Sci. 105, 1541–1549. https://doi.org/10.1111/cas.12548

Kavian, N., Marut, W., Servettaz, A., Nicco, C., Chéreau, C., Lemaréchal, H., Borderie, D., Dupin, N., Weill, B., Batteux, F., 2012. Reactive oxygen species-mediated killing of activated fibroblasts by arsenic trioxide ameliorates fibrosis in a murine model of systemic sclerosis. Arthritis Rheum. 64, 3430–3440. https://doi.org/10.1002/art.34534

Kim, Seokuee, Kim, Sujong, Park, Y.S., Park, J.O., Lim, H.Y., Ahn, J.S., Lee, J., Sun, J.M., Kang, W.K., Han, R., Kim, J., Ahn, M.-J., 2020. Phase I clinical trial of KML001 monotherapy in patients with advanced solid tumors. Expert Opin. Investig. Drugs 29, 1059–1067. https://doi.org/10.1080/13543784.2020.1804855

King, T.E., Bradford, W.Z., Castro-Bernardini, S., Fagan, E.A., Glaspole, I., Glassberg, M.K., Gorina, E., Hopkins, P.M., Kardatzke, D., Lancaster, L., Lederer, D.J., Nathan, S.D., Pereira, C.A., Sahn, S.A., Sussman, R., Swigris, J.J., Noble, P.W., ASCEND Study Group, 2014. A phase 3 trial of pirfenidone in

ACCEPTED MANUSCRIPT - CLEAN COPY

patients with idiopathic pulmonary fibrosis. N. Engl. J. Med. 370, 2083–2092. https://doi.org/10.1056/NEJMoa1402582

King, T.E., Pardo, A., Selman, M., 2011. Idiopathic pulmonary fibrosis. Lancet Lond. Engl. 378, 1949–1961. https://doi.org/10.1016/S0140-6736(11)60052-4

Kumana, C.R., Au, W.Y., Lee, N.S.L., Kou, M., Mak, R.W.M., Lam, C.W., Kwong, Y.L., 2002. Systemic availability of arsenic from oral arsenic-trioxide used to treat patients with hematological malignancies. Eur. J. Clin. Pharmacol. 58, 521–526. https://doi.org/10.1007/s00228-002-0514-x

Kurowska-Stolarska, M., Hasoo, M.K., Welsh, D.J., Stewart, L., McIntyre, D., Morton, B.E., Johnstone, S., Miller, A.M., Asquith, D.L., Millar, N.L., Millar, A.B., Feghali-Bostwick, C.A., Hirani, N., Crick, P.J., Wang, Y., Griffiths, W.J., McInnes, I.B., McSharry, C., 2017. The role of microRNA-155/liver X receptor pathway in experimental and idiopathic pulmonary fibrosis. J. Allergy Clin. Immunol. 139, 1946–1956. https://doi.org/10.1016/j.jaci.2016.09.021

Lederer, D.J., Martinez, F.J., 2018. Idiopathic Pulmonary Fibrosis. N. Engl. J. Med. 378, 1811–1823. https://doi.org/10.1056/NEJMra1705751

Liu, S.H., Yang, R.-S., Yen, Y.-P., Chiu, C.-Y., Tsai, K.-S., Lan, K.-C., 2015. Low-Concentration Arsenic Trioxide Inhibits Skeletal Myoblast Cell Proliferation via a Reactive Oxygen Species-Independent Pathway. PloS One 10, e0137907. https://doi.org/10.1371/journal.pone.0137907

Luo, F., Zhuang, Y., Sides, M.D., Sanchez, C.G., Shan, B., White, E.S., Lasky, J.A., 2014. Arsenic trioxide inhibits transforming growth factor-β1-induced fibroblast to myofibroblast differentiation in vitro and bleomycin induced lung fibrosis in vivo. Respir. Res. 15, 51. https://doi.org/10.1186/1465-9921-15-51

Maghmomeh, A.O., El-Gayar, A.M., El-Karef, A., Abdel-Rahman, N., 2020. Arsenic trioxide and curcumin attenuate cisplatin-induced renal fibrosis in rats through targeting Hedgehog signaling. Naunyn. Schmiedebergs Arch. Pharmacol. 393, 303–313. https://doi.org/10.1007/s00210-019-01734-y

Marchand-Adam, S., Marchal, J., Cohen, M., Soler, P., Gerard, B., Castier, Y., Lesèche, G., Valeyre, D., Mal, H., Aubier, M., Dehoux, M., Crestani, B., 2003. Defect of hepatocyte growth factor secretion by fibroblasts in idiopathic pulmonary fibrosis. Am. J. Respir. Crit. Care Med. 168, 1156–1161. https://doi.org/10.1164/rccm.200212-1514OC

Matsuoka, H., Arai, T., Mori, M., Goya, S., Kida, H., Morishita, H., Fujiwara, H., Tachibana, I., Osaki, T., Hayashi, S., 2002. A p38 MAPK inhibitor, FR-167653, ameliorates murine bleomycin-induced pulmonary fibrosis. Am. J. Physiol. Lung Cell. Mol. Physiol. 283, L103-112. https://doi.org/10.1152/ajplung.00187.2001

Morales, A.A., Gutman, D., Cejas, P.J., Lee, K.P., Boise, L.H., 2009. Reactive oxygen species are not required for an arsenic trioxide-induced antioxidant response or apoptosis. J. Biol. Chem. 284, 12886–12895. https://doi.org/10.1074/jbc.M806546200

Oh, C.J., Kim, J.-Y., Min, A.-K., Park, K.-G., Harris, R.A., Kim, H.-J., Lee, I.-K., 2012. Sulforaphane attenuates hepatic fibrosis via NF-E2-related factor 2-mediated inhibition of transforming growth factor-β/Smad signaling. Free Radic. Biol. Med. 52, 671–682. https://doi.org/10.1016/j.freeradbiomed.2011.11.012

ACCEPTED MANUSCRIPT - CLEAN COPY

Park, J.W., Choi, Y.J., Jang, M.A., Baek, S.H., Lim, J.H., Passaniti, T., Kwon, T.K., 2001. Arsenic trioxide induces G2/M growth arrest and apoptosis after caspase-3 activation and bcl-2 phosphorylation in promonocytic U937 cells. Biochem. Biophys. Res. Commun. 286, 726–734. https://doi.org/10.1006/bbrc.2001.5416

Plataki, M., Cho, S.J., Harris, R.M., Huang, H.-R., Yun, H.S., Schiffer, K.T., Stout-Delgado, H.W., 2019. Mitochondrial Dysfunction in Aged Macrophages and Lung during Primary Streptococcus pneumoniae Infection is Improved with Pirfenidone. Sci. Rep. 9, 971. https://doi.org/10.1038/s41598-018-37438-1

Raghu, G., Remy-Jardin, M., Myers, J.L., Richeldi, L., Ryerson, C.J., Lederer, D.J., Behr, J., Cottin, V., Danoff, S.K., Morell, F., Flaherty, K.R., Wells, A., Martinez, F.J., Azuma, A., Bice, T.J., Bouros, D., Brown, K.K., Collard, H.R., Duggal, A., Galvin, L., Inoue, Y., Jenkins, R.G., Johkoh, T., Kazerooni, E.A., Kitaichi, M., Knight, S.L., Mansour, G., Nicholson, A.G., Pipavath, S.N.J., Buendía-Roldán, I., Selman, M., Travis, W.D., Walsh, S., Wilson, K.C., American Thoracic Society, European Respiratory Society, Japanese Respiratory Society, and Latin American Thoracic Society, 2018. Diagnosis of Idiopathic Pulmonary Fibrosis. An Official ATS/ERS/JRS/ALAT Clinical Practice Guideline. Am. J. Respir. Crit. Care Med. 198, e44–e68. https://doi.org/10.1164/rccm.201807-1255ST

Rangarajan, S., Kurundkar, A., Kurundkar, D., Bernard, K., Sanders, Y.Y., Ding, Q., Antony, V.B., Zhang, J., Zmijewski, J., Thannickal, V.J., 2016. Novel Mechanisms for the Antifibrotic Action of Nintedanib. Am. J. Respir. Cell Mol. Biol. 54, 51–59. https://doi.org/10.1165/rcmb.2014-0445OC

Richeldi, L., du Bois, R.M., Raghu, G., Azuma, A., Brown, K.K., Costabel, U., Cottin, V., Flaherty, K.R., Hansell, D.M., Inoue, Y., Kim, D.S., Kolb, M., Nicholson, A.G., Noble, P.W., Selman, M., Taniguchi, H., Brun, M., Le Maulf, F., Girard, M., Stowasser, S., Schlenker-Herceg, R., Disse, B., Collard, H.R., INPULSIS Trial Investigators, 2014. Efficacy and safety of nintedanib in idiopathic pulmonary fibrosis. N. Engl. J. Med. 370, 2071–2082. https://doi.org/10.1056/NEJMoa1402584

Richeldi, L., Kolb, M., Jouneau, S., Wuyts, W.A., Schinzel, B., Stowasser, S., Quaresma, M., Raghu, G., 2020. Efficacy and safety of nintedanib in patients with advanced idiopathic pulmonary fibrosis. BMC Pulm. Med. 20, 3. https://doi.org/10.1186/s12890-019-1030-4

Ruwanpura, S.M., Thomas, B.J., Bardin, P.G., 2020. Pirfenidone: Molecular Mechanisms and Potential Clinical Applications in Lung Disease. Am. J. Respir. Cell Mol. Biol. 62, 413–422. https://doi.org/10.1165/rcmb.2019-0328TR

Shen, Y., Shen, Z.X., Yan, H., Chen, J., Zeng, X.Y., Li, J.M., Li, X.S., Wu, W., Xiong, S.M., Zhao, W.L., Tang, W., Wu, F., Liu, Y.F., Niu, C., Wang, Z.Y., Chen, S.J., Chen, Z., 2001. Studies on the clinical efficacy and pharmacokinetics of low-dose arsenic trioxide in the treatment of relapsed acute promyelocytic leukemia: a comparison with conventional dosage. Leukemia 15, 735–741. https://doi.org/10.1038/sj.leu.2402106

Shen, Z.-X., Chen, G.-Q., Ni, J.-H., Li, X.-S., Xiong, S.-M., Qiu, Q.-Y., Zhu, J., Tang, W., Sun, G.-L., Yang, K.-Q., Chen, Y., Zhou, L., Fang, Z.-W., Wang, Y.-T., Ma, J., Zhang, P., Zhang, T.-D., Chen, S.-J., Chen, Z., Wang, Z.-Y., 1997. Use of Arsenic Trioxide (As2O3) in the Treatment of Acute Promyelocytic Leukemia (APL): II. Clinical Efficacy and Pharmacokinetics in Relapsed Patients. Blood 89, 3354–3360. https://doi.org/10.1182/blood.V89.9.3354

Shi, Y., Cao, T., Huang, H., Lian, C., Yang, Y., Wang, Z., Ma, J., Xia, J., 2017. Arsenic trioxide inhibits cell growth and motility via up-regulation of let-7a in breast cancer cells. Cell Cycle Georget. Tex 16, 2396–2403. https://doi.org/10.1080/15384101.2017.1387699

ACCEPTED MANUSCRIPT - CLEAN COPY

Soignet, S.L., Frankel, S.R., Douer, D., Tallman, M.S., Kantarjian, H., Calleja, E., Stone, R.M., Kalaycio, M., Scheinberg, D.A., Steinherz, P., Sievers, E.L., Coutré, S., Dahlberg, S., Ellison, R., Warrell, R.P., 2001. United States multicenter study of arsenic trioxide in relapsed acute promyelocytic leukemia. J. Clin. Oncol. Off. J. Am. Soc. Clin. Oncol. 19, 3852–3860. https://doi.org/10.1200/JCO.2001.19.18.3852

Su, Y., Jiang, C., Zhang, L., Wang, F., 2015. Arsenic Trioxide Inhibits Proliferation of Rabbit Tenon's Capsule Fibroblasts After Trabeculectomy by Downregulating Expression of Extracellular Matrix Proteins. Invest. Ophthalmol. Vis. Sci. 56, 6663–6670. https://doi.org/10.1167/iovs.15-17289

Suganuma, H., Sato, A., Tamura, R., Chida, K., 1995. Enhanced migration of fibroblasts derived from lungs with fibrotic lesions. Thorax 50, 984–989. https://doi.org/10.1136/thx.50.9.984

Tangkijvanich, P., Santiskulvong, C., Melton, A.C., Rozengurt, E., Yee, H.F., 2002. p38 MAP kinase mediates platelet-derived growth factor-stimulated migration of hepatic myofibroblasts. J. Cell. Physiol. 191, 351–361. https://doi.org/10.1002/jcp.10112

Tingting, R., Wei, G., Changliang, P., Xinchang, L., Yi, Y., 2010. Arsenic trioxide inhibits osteosarcoma cell invasiveness via MAPK signaling pathway. Cancer Biol. Ther. 10, 251–257. https://doi.org/10.4161/cbt.10.3.12349

Upagupta, C., Shimbori, C., Alsilmi, R., Kolb, M., 2018. Matrix abnormalities in pulmonary fibrosis. Eur. Respir. Rev. Off. J. Eur. Respir. Soc. 27, 180033. https://doi.org/10.1183/16000617.0033-2018

Wang, L., Kou, M.-C., Weng, C.-Y., Hu, L.-W., Wang, Y.-J., Wu, M.-J., 2012. Arsenic modulates heme oxygenase-1, interleukin-6, and vascular endothelial growth factor expression in endothelial cells: roles of ROS, NF-κB, and MAPK pathways. Arch. Toxicol. 86, 879–896. https://doi.org/10.1007/s00204-012-0845-z

Wei, J., Zhu, H., Lord, G., Bhattachayya, M., Jones, B.M., Allaway, G., Biswal, S.S., Korman, B., Marangoni, R.G., Tourtellotte, W.G., Varga, J., 2017. Nrf2 exerts cell-autonomous antifibrotic effects: compromised function in systemic sclerosis and therapeutic rescue with a novel heterocyclic chalcone derivative. Transl. Res. J. Lab. Clin. Med. 183, 71-86.e1. https://doi.org/10.1016/j.trsl.2016.12.002

Wei, L.-H., Lai, K.-P., Chen, C.-A., Cheng, C.-H., Huang, Y.-J., Chou, C.-H., Kuo, M.-L., Hsieh, C.-Y., 2005. Arsenic trioxide prevents radiation-enhanced tumor invasiveness and inhibits matrix metalloproteinase-9 through downregulation of nuclear factor kappaB. Oncogene 24, 390–398. https://doi.org/10.1038/sj.onc.1208192

Wollin, L., Wex, E., Pautsch, A., Schnapp, G., Hostettler, K.E., Stowasser, S., Kolb, M., 2015. Mode of action of nintedanib in the treatment of idiopathic pulmonary fibrosis. Eur. Respir. J. 45, 1434–1445. https://doi.org/10.1183/09031936.00174914

Yamaguchi, H., Igarashi, M., Hirata, A., Susa, S., Ohnuma, H., Tominaga, M., Daimon, M., Kato, T., 2001. Platelet-derived growth factor BB-induced p38 mitogen-activated protein kinase activation causes cell growth, but not apoptosis, in vascular smooth muscle cells. Endocr. J. 48, 433–442. https://doi.org/10.1507/endocrj.48.433

Yang, L., Qu, M., Wang, Yao, Duan, H., Chen, P., Wang, Ye, Shi, W., Danielson, P., Zhou, Q., 2013. Trichostatin A inhibits transforming growth factor-β-induced reactive oxygen species accumulation and myofibroblast differentiation via enhanced NF-E2-related factor 2-antioxidant response element signaling. Mol. Pharmacol. 83, 671–680. https://doi.org/10.1124/mol.112.081059

ACCEPTED MANUSCRIPT - CLEAN COPY

Yang, M.-H., Chang, K.-J., Zheng, J.-C., Huang, H., Sun, G.-Y., Zhao, X.-W., Li, B., Xiu, Q.-Y., 2017. Anti-angiogenic effect of arsenic trioxide in lung cancer via inhibition of endothelial cell migration, proliferation and tube formation. Oncol. Lett. 14, 3103–3109. https://doi.org/10.3892/ol.2017.6518

Zhang, F., Duan, J., Song, H., Yang, L., Zhou, M., Wang, X., 2020. Combination of canstatin and arsenic trioxide suppresses the development of hepatocellular carcinoma. Drug Dev. Res. https://doi.org/10.1002/ddr.21766

Zhang, L., Liu, L., Zhan, S., Chen, L., Wang, Y., Zhang, Y., Du, J., Wu, Y., Gu, L., 2018. Arsenic Trioxide Suppressed Migration and Angiogenesis by Targeting FOXO3a in Gastric Cancer Cells. Int. J. Mol. Sci. 19. https://doi.org/10.3390/ijms19123739

Zhang, S., Ma, C., Pang, H., Zeng, F., Cheng, L., Fang, B., Ma, J., Shi, Y., Hong, H., Chen, J., Wang, Z., Xia, J., 2016. Arsenic trioxide suppresses cell growth and migration via inhibition of miR-27a in breast cancer cells. Biochem. Biophys. Res. Commun. 469, 55–61. https://doi.org/10.1016/j.bbrc.2015.11.071

Zhao, S., Tsuchida, T., Kawakami, K., Shi, C., Kawamoto, K., 2002. Effect of As2O3 on cell cycle progression and cyclins D1 and B1 expression in two glioblastoma cell lines differing in p53 status. Int. J. Oncol. 21, 49–55.

Zhong, L., Hao, H., Chen, D., Hou, Q., Zhu, Z., He, W., Sun, S., Sun, M., Li, M., Fu, X., 2019. Arsenic trioxide inhibits the differentiation of fibroblasts to myofibroblasts through nuclear factor erythroid 2-like 2 (NFE2L2) protein and the Smad2/3 pathway. J. Cell. Physiol. 234, 2606–2617. https://doi.org/10.1002/jcp.27073

Zhuo, Y., Zhang, J., Laboy, M., Lasky, J.A., 2004. Modulation of PDGF-C and PDGF-D expression during bleomycin-induced lung fibrosis. Am. J. Physiol. Lung Cell. Mol. Physiol. 286, L182-188. https://doi.org/10.1152/ajplung.00083.2003

ACCEPTED MANUSCRIPT - CLEAN COPY

13. Figure Legends

Figure 1: ATO reduces HLF proliferation. IPF and control HLFs were treated with 0.01-1 µM ATO alone for 72 h (A-B) or with 0.01-1 µM ATO for 24 h and then stimulated with 50 ng/ml PDGF-BB for 72 h (C-D). The proliferation of unstimulated and PDGF-BB-stimulated cells were determined by fluorescent acridine orange/propidium iodide staining and automated fluorescence cell counting. After cell counting, the relative cell proliferation was calculated by dividing the number of viable cells exposed to ATO +/- PDGF-BB by the number of viable untreated cells, which was arbitrarily set at 1. All results are expressed as means ± SEM of 6 independent experiments. Significant differences were determined by Student's *t*-test ($ $p<0.05$) or by ANOVA followed by the Dunnett's multiple comparison *t*-test (** $p<0.01$; *** $p<0.001$).

Figure 2: ATO alters cell cycle distribution in IPF HLFs. IPF HLFs were treated with 1 µM ATO for 24 h and then stimulated with 50 ng/ml PDGF-BB for 72 h (A-B) or 24 h (C-D). **A-B.** Cells were washed, fixed and stained with propidium iodide to analyse the cell cycle by flow cytometry. **A:** Representative graphs saved during flow cytometry analysis. **B:** Data for each cell cycle phase expressed as percentages of total IPF HLFs. **C:** Representative Western blot showing the cell cycle-related proteins in IPF HLFs. **D:** Proteins quantified by densitometry and normalized to the GAPDH. The fold change in protein expression measured in treated and stimulated cells was determined by arbitrarily setting at 1 the protein expression measured in untreated cells. **B, D:** Results are expressed as means ± SEM of 7 (B) and 4-9 (D) independent experiments. Significant differences were determined by Student's *t*-test ($ $p<0.05$).

ACCEPTED MANUSCRIPT - CLEAN COPY

Figure 3: ATO blocks the PDGF-BB-induced migration of IPF and control HLFs. IPF (A) and control (B) HLFs were treated with ATO for 24 h and 25 ng/ml PDGF-BB was used as a chemoattractant to induce cell migration. Values are expressed relative to the migration of untreated HLFs (arbitrarily set at 1). Results are expressed as with means ± SEM of 6 (IPF) and 5 (Control) independent experiments. Significant differences were determined by Student's *t*-test ($ $p<0.05$) or by ANOVA followed by the Dunnett's multiple comparison *t*-test (** $p<0.01$; *** $p<0.001$).

Figure 4: ATO reduces PDGF-BB-induced p38-kinase phosphorylation. IPF and control HLFs were treated with 0.01-1 µM ATO for 24 h and then stimulated with 50 ng/ml PDGF-BB for 10 min. **A.** Representative Western blots showing the phosphorylation of PDGFR, ERK, AKT and p38-kinase in IPF HLFs. **B**. Proteins were quantified by densitometry and then normalized to GAPDH. The fold change in the levels of phosphorylated proteins found in stimulated cells was determined by arbitrarily setting at 1 the levels of phosphorylated proteins measured in untreated cells. Results are expressed as with means ± SEM of 5-8 independent experiments. Significant differences were determined by Student's *t*-test ($ $p<0.05$; $$ $p<0.01$), or by ANOVA followed by the Dunnett's multiple comparison *t*-test ** $p<0.01$).

Figure 5: ATO decreases TGF-β1-induced cell differentiation in IPF and control HLF. IPF and control HLFs were treated with 0.01-1 µM ATO for 24 h and stimulated with 1 ng/ml TGF-β1 for a further 24 h. **A, C.** Representative Western blots of collagen-1 (COL1) and α-SMA. **B, D**. Proteins were quantified by densitometry and normalized to the GAPDH. The fold change in protein expression in stimulated cells was determined by arbitrarily setting at 1

ACCEPTED MANUSCRIPT - CLEAN COPY

the protein expression measured in untreated cells. Results are expressed as with means ± SEM of 8-10 (IPF) and 5-6 (Control) independent experiments. Significant differences were determined by Student's *t*-test ($ $p<0.05$; $$ $p<0.01$), or by ANOVA followed by the Dunnett's multiple comparison *t*-test (* $p<0.05$; ** $p<0.01$).

Figure 6: ATO prevents the phosphorylation of SMAD2/3 induced by TGF-β1 in IPF and control HLFs. A, C. Representative Western blots showing the phosphorylation of SMAD2 and SMAD3 in IPF (A) and control (C) HLFs treated with 0.01-1 µM ATO for 24 h and then stimulated with 1 ng/ml TGF-β1 for 30 min. **B, D**. Proteins were quantified by densitometry and then normalized to the GAPDH. The fold change in the levels of phosphorylated proteins found in stimulated cells was determined by arbitrarily setting at 1 the levels of phosphorylated proteins measured in untreated cells. Results are expressed as means ± SEM of 4-7 (B) and 4-5 (D) independent experiments. Significant differences were determined by Student's t-test ($ $p<0.05$), or by ANOVA followed by Dunnett's multiple comparison t-test (* $p<0.05$; ** $p<0.01$).

Figure 7: ATO induces the expression of NRF2 and antioxidant proteins in IPF HLFs.

IPF HLFs were treated with 0.1-0.5 µM ATO for the indicated times (A) or for 24 h (C, E) and then stimulated with TGF-β1 for 24 h or left unstimulated (E). **A, C, E.** Representative Western blots of NRF2, HO-1 and NQO-1. **B, D, F**. Proteins were quantified by densitometry and normalized to the GAPDH. The fold change in protein expression found in treated and/or stimulated cells was determined by arbitrarily setting at 1 the protein expression measured in untreated cells. Results are expressed as means ± SEM of 3 (B), 6-7 (D) and 5-8 (E)

ACCEPTED MANUSCRIPT - CLEAN COPY

independent experiments. Significant differences were determined by ANOVA followed by the Dunnett's multiple comparison t-test (* $p<0.05$; ** $p<0.01$; ***$p<0.001$).

Figure 8: NRF2 does not mediate the ATO-dependent inhibition of α-SMA expression induced by TGF-β1. IPF HLFs were transfected with control-siRNA (si ctrl) or NRF2-siRNA (si Nrf2) for 8 h. They were then incubated with 1 µM ATO for 24 h and stimulated with TGF-β1 (1 ng/ml) for a further 24 h. Relative *NRF2*, *NQO1* and *ACTA2* mRNA levels were measured by quantitative RT-PCR and normalized to that of endogenous ribosomal *18S* RNA. The fold change in mRNA concentrations measured in treated and/or stimulated HLFs was determined by arbitrarily setting at 1 mRNA concentrations measured in unstimulated HLFs transfected with si ctrl. Results are expressed as with means ± SEM of 5 independent experiments. Significant differences were determined by Student's *t*-test ($ $p<0.05$; $$ $p<0.01$) or by ANOVA followed by Dunnett's multiple comparison t-test (* $p<0.05$; ** $p<0.01$; *** $p<0.001$).

ACCEPTED MANUSCRIPT - CLEAN COPY

Credit author statement

LV, SJ, AJ conceived and designed the study. AJ, LV, SJ revised the manuscript. AJ, CM, MD performed the experiments. AJ, LV, SJ analyzed and interpreted the data. FLG, DCC, CLN, BDLT, SR provided lung biopsy. AJ, LV, SJ, LW wrote the paper. All authors read and approved the final revised manuscript.

ACCEPTED MANUSCRIPT - CLEAN COPY

Declaration of interests

☐The authors declare that they have no known competing financial interests or personal relationships that could have appeared to influence the work reported in this paper.

☒The authors declare the following financial interests/personal relationships which may be considered as potential competing interests:

Laurent Vernhet reports financial support was provided by Boehringer Ingelheim Pharma GmbH and Co KG. Lutz Wollin reports a relationship with Boehringer Ingelheim Pharma GmbH and Co KG Biberach that includes: employment.

ACCEPTED MANUSCRIPT - CLEAN COPY

Highlights

- ATO counteracted pro-fibrotic activities of primary IPF and control Human Lung Fibroblasts (HLFs).
- ATO prevented the PDGF-BB-induced proliferation of IPF and control HLFs
- ATO prevented the PDGF-BB-induced migration of IPF and control HLFs.
- ATO decreased the TGFβ-1-induced differentiation of HLFs.
- ATO induced NRF2 and antioxidant proteins in IPF and control HLFs

ACCEPTED MANUSCRIPT - CLEAN COPY

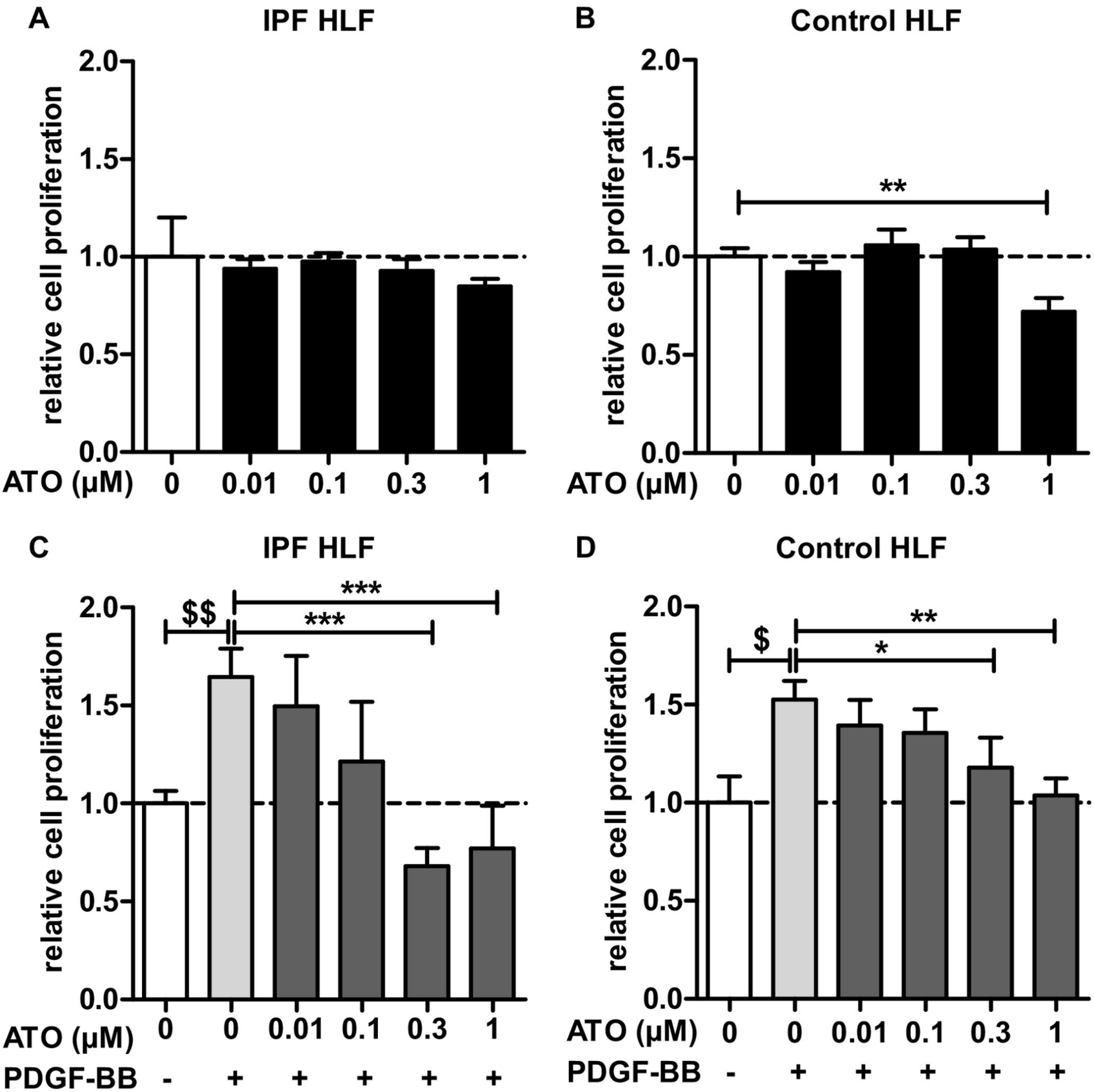

ACCEPTED MANUSCRIPT - CLEAN COPY

Figure 1

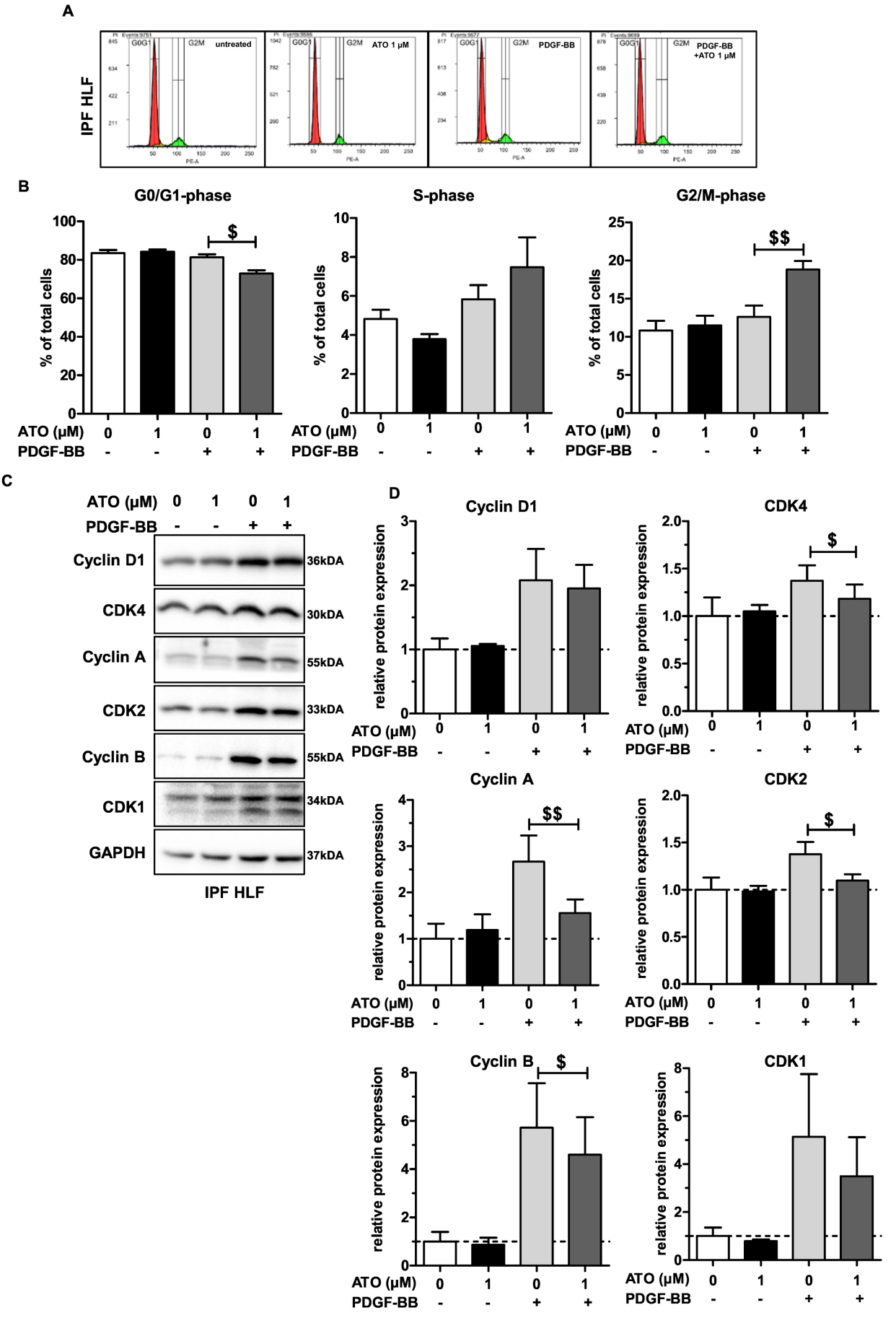

ACCEPTED MANUSCRIPT - CLEAN COPY

Figure 2

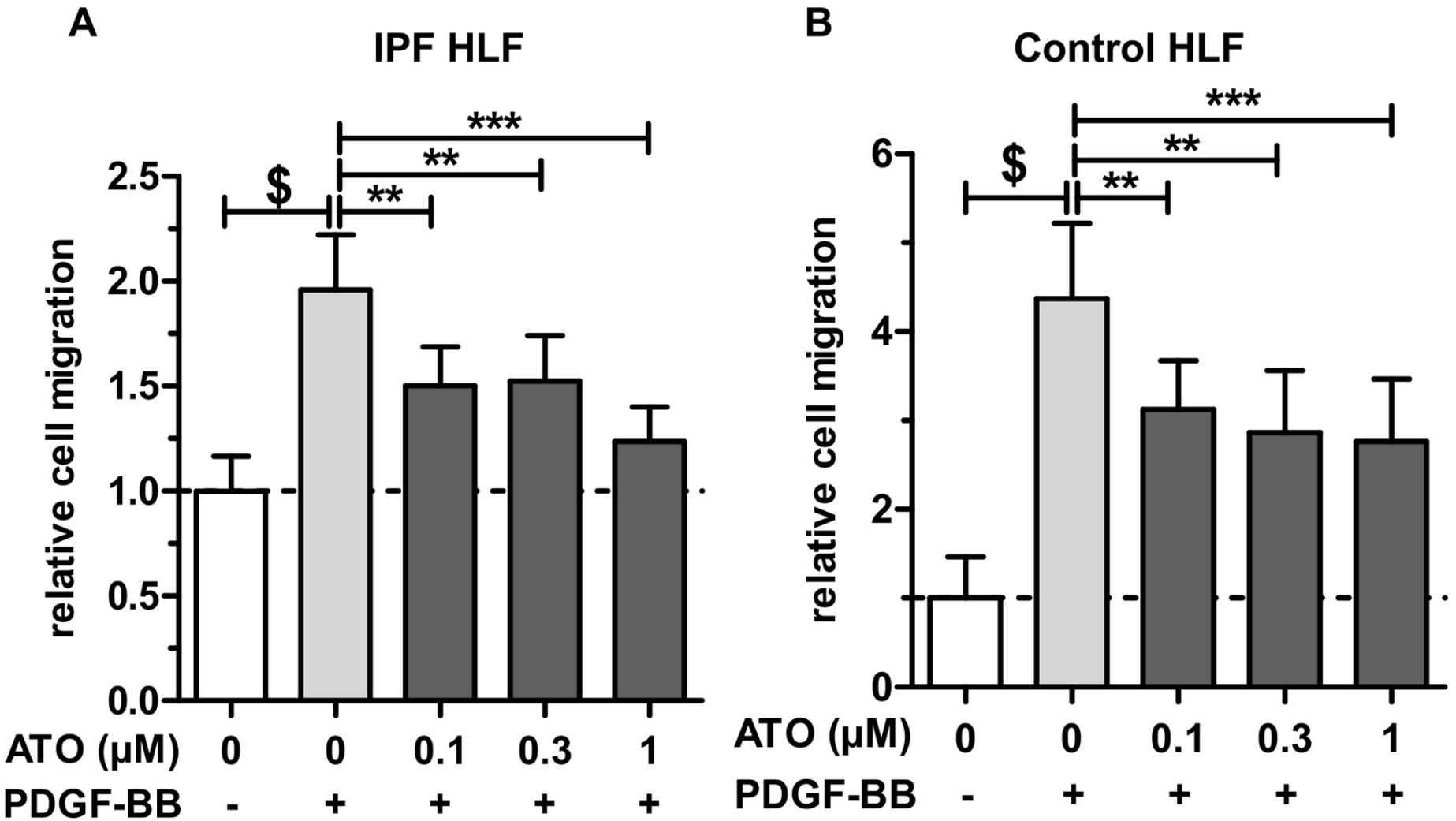

ACCEPTED MANUSCRIPT - CLEAN COPY

Figure 3

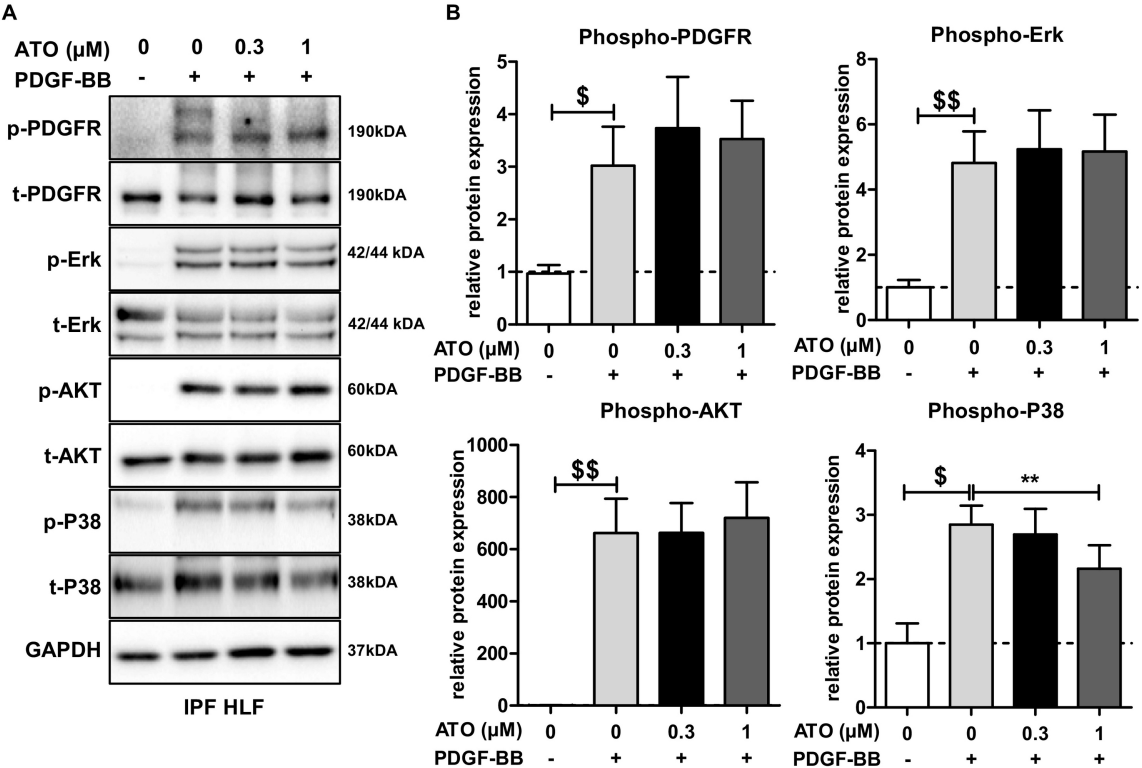

ACCEPTED MANUSCRIPT - CLEAN COPY

Figure 4

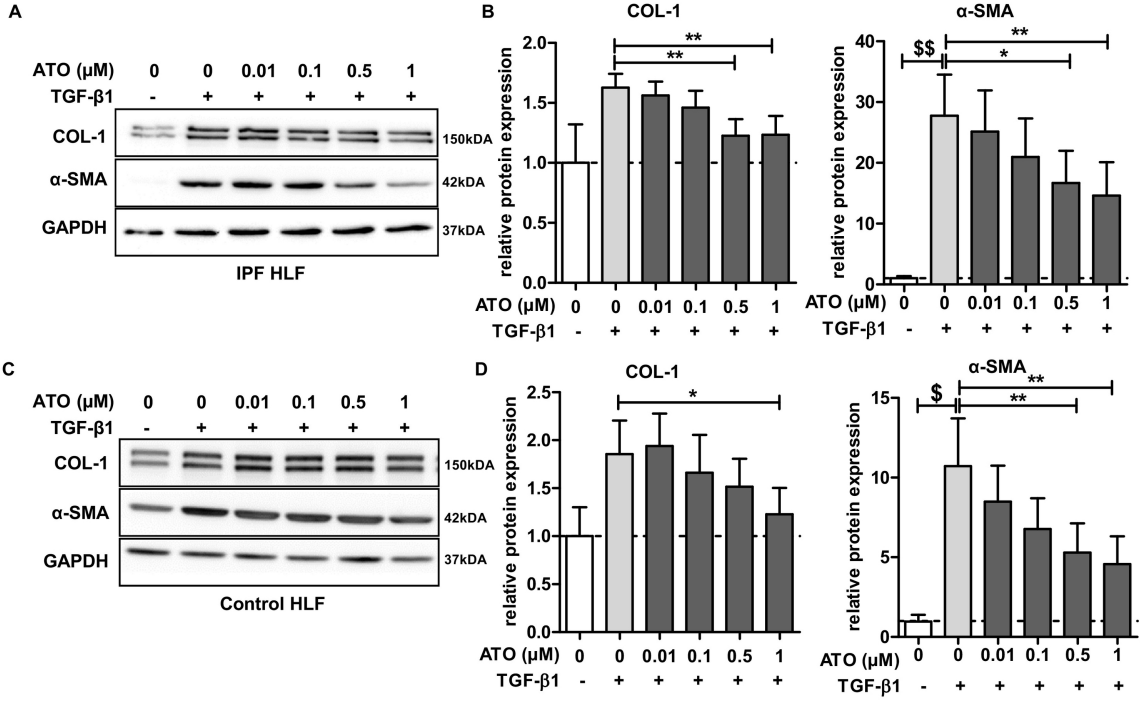

ACCEPTED MANUSCRIPT - CLEAN COPY

Figure 5

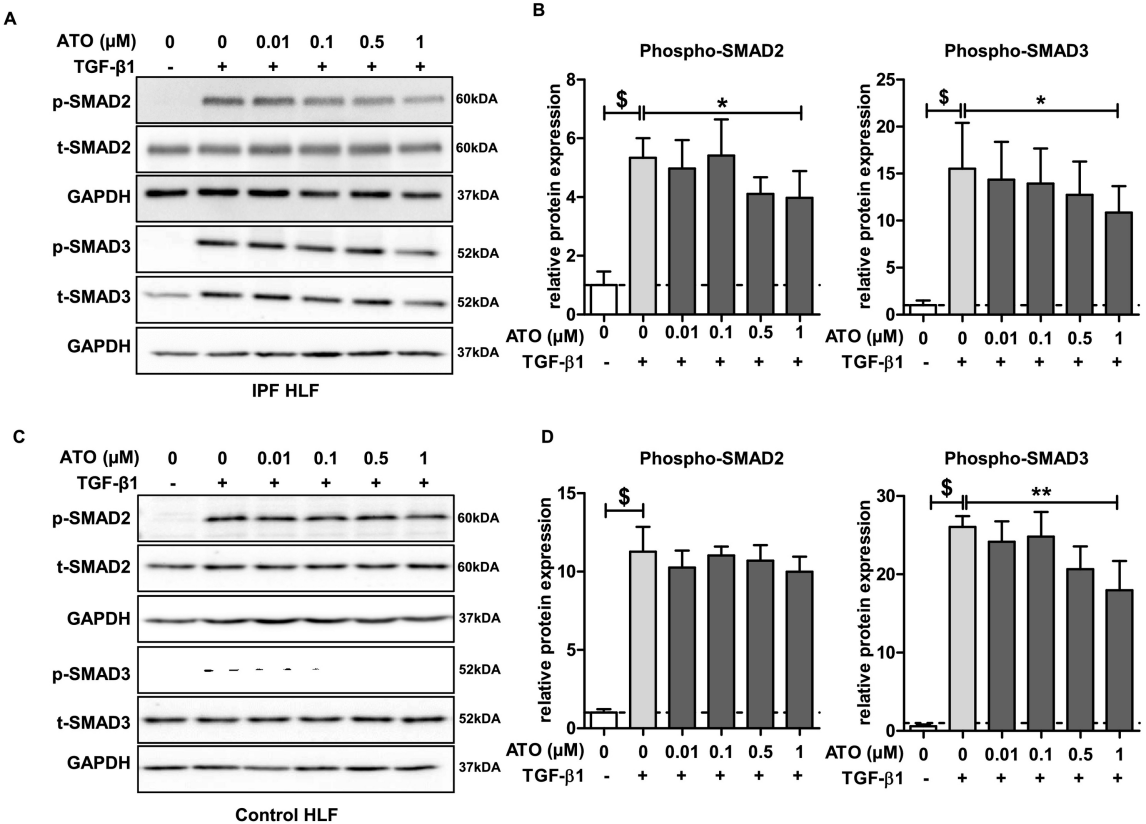

ACCEPTED MANUSCRIPT - CLEAN COPY

Figure 6

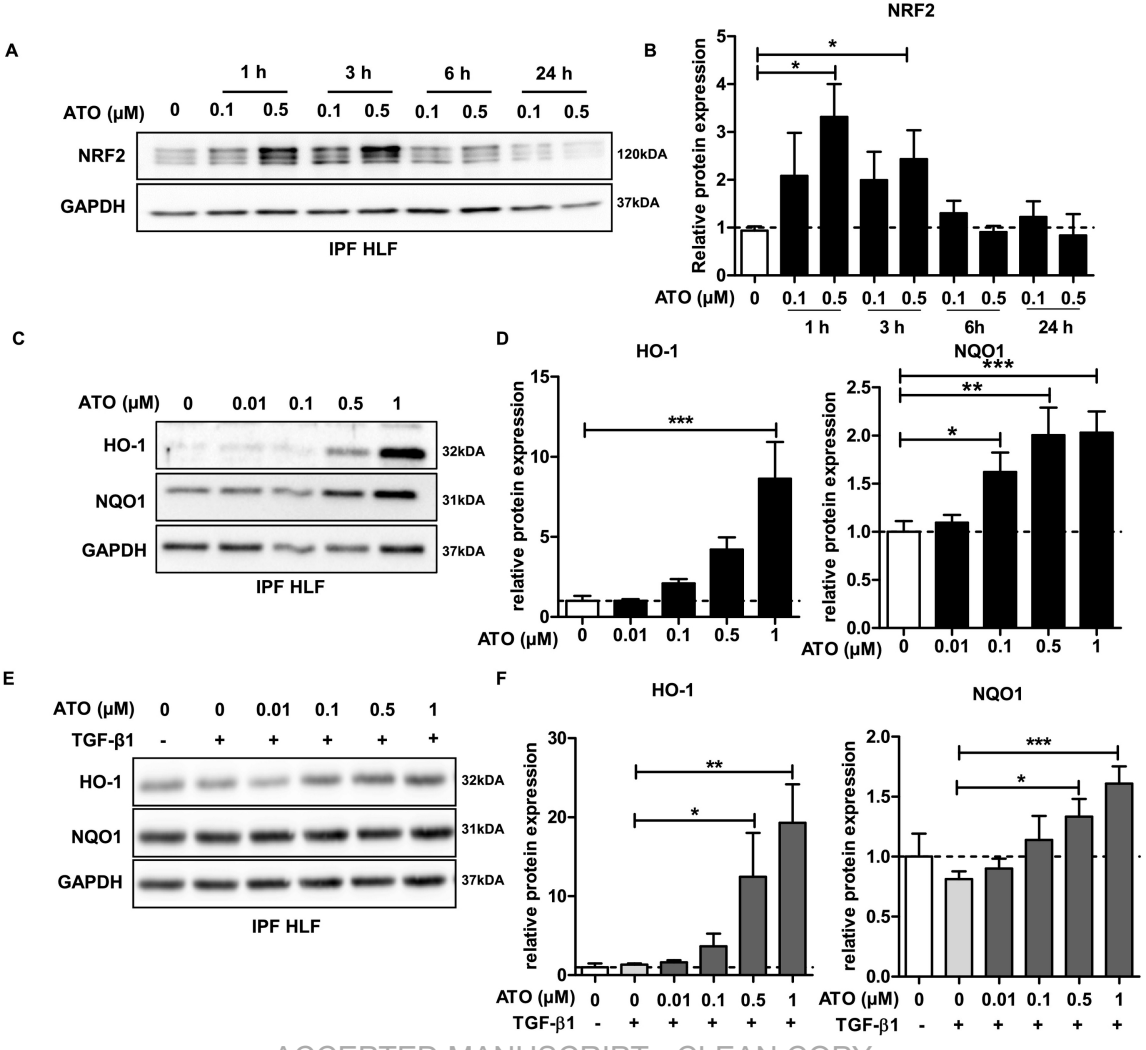

ACCEPTED MANUSCRIPT - CLEAN COPY

Figure 7

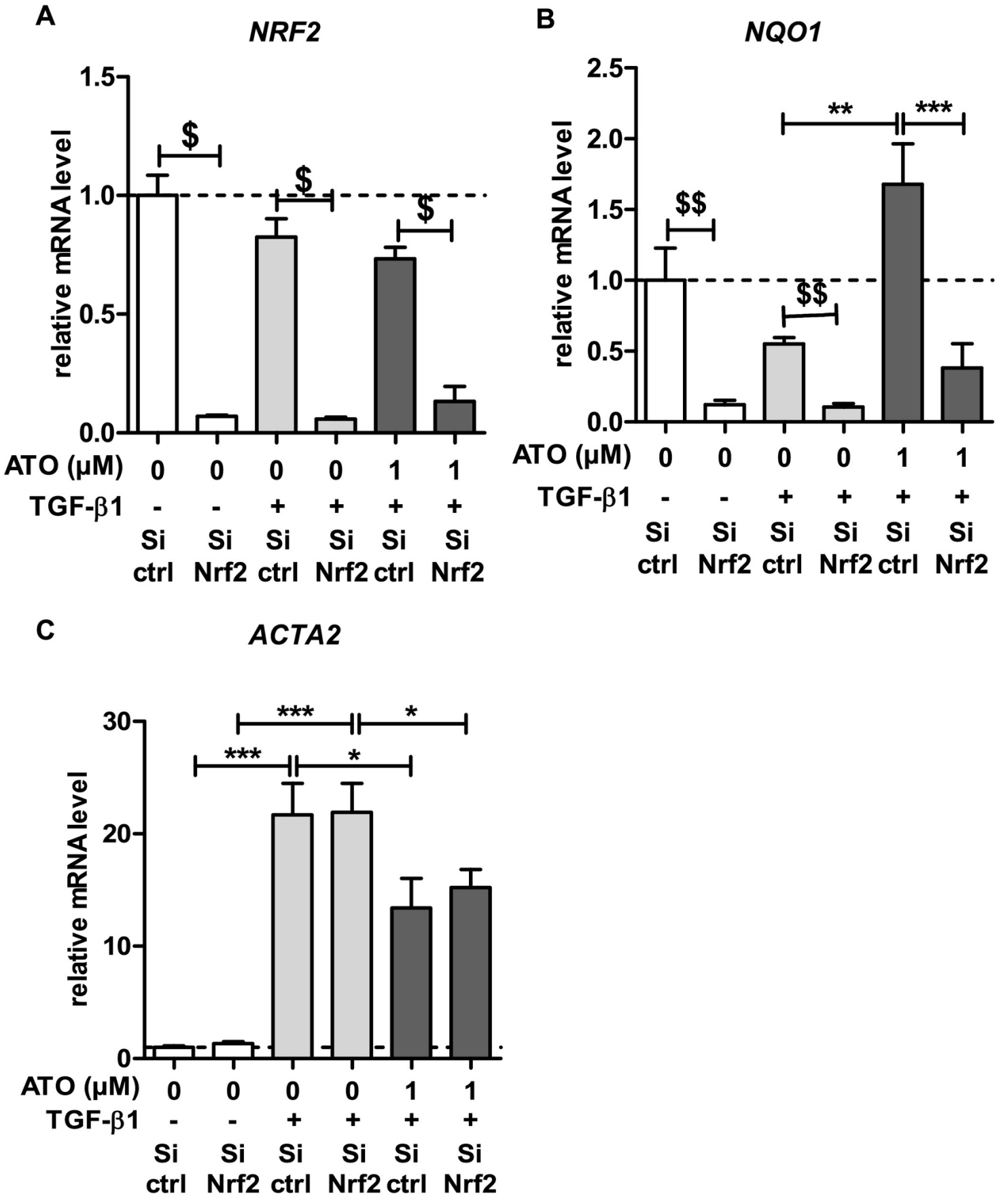

ACCEPTED MANUSCRIPT - CLEAN COPY

Figure 8